Noninvasive Measurement of Intra-Aneurysmal Pressure and Flow Pattern Using Phase Contrast with Vastly Undersampled Isotropic Projection Imaging

R. Moftakhar, B. Aagaard-Kienitz, K. Johnson, P.A. Turski, A.S. Turk, D.B. Niemann, D. Consigny, J. Grinde, O. Wieben and C.A. Mistretta

AJNR Am J Neuroradiol 2007, 28 (9) 1710-1714
doi: https://doi.org/10.3174/ajnr.A0648
http://www.ajnr.org/content/28/9/1710

ORIGINAL RESEARCH

Noninvasive Measurement of Intra-Aneurysmal Pressure and Flow Pattern Using Phase Contrast with Vastly Undersampled Isotropic Projection Imaging

R. Moftakhar
B. Aagaard-Kienitz
K. Johnson
P.A. Turski
A.S. Turk
D.B. Niemann
D. Consigny
J. Grinde
O. Wieben
C.A. Mistretta

BACKGROUND AND PURPOSE: Currently, more reliable parameters to predict the risk of aneurysmal rupture are needed. Intra-aneurysmal pressure gradients and flow maps could provide additional information regarding the risk of rupture. Our hypothesis was that phase contrast with vastly undersampled isotropic projection reconstruction (PC-VIPR), a novel 3D MR imaging sequence, could accurately assess intra-aneurysmal pressure gradients in a canine aneurysmal model when compared with invasive measurements.

MATERIALS AND METHODS: A total of 13 surgically created aneurysms in 8 canines were included in this study. Pressure measurements were performed in the parent vessel, aneurysm neck, and 5 regions within the aneurysmal sac with a microcatheter. PC-VIPR sequence was used to obtain cardiac-gated velocity measurements in a region covering the entire aneurysm. The velocity and pressure gradient maps derived from the PC-VIPR data were then coregistered with the anatomic DSA images and compared with catheter measurements.

RESULTS: In 7 of the bifurcation aneurysms, the velocity flow maps demonstrated a recirculation flow pattern with a small neck-to-dome pressure gradient (mean, +0.5 mm Hg). In 1 bifurcation aneurysm, a flow jet extending from the neck to the dome with significantly greater pressure gradient (+50.2 mm Hg) was observed. All sidewall aneurysms had low flow in the sac with intermediate pressure gradients (mean, +8.3 mm Hg). High statistical correlation existed between PC-VIPR aneurysmal pressures and microcatheter pressure measurements ($R = 0.82$, $P < .01$).

CONCLUSION: PC-VIPR can provide anatomic as well as noninvasive quantitative and qualitative hemodynamic information in the canine aneurysm model. The PC-VIPR intra-aneurysmal pressure measurements correlated well with catheter measurements.

The natural history of unruptured aneurysms remains controversial and poorly understood. The largest prospective study regarding the natural history of unruptured aneurysms concluded that the cumulative 5-year risk of rupture for aneurysms less than 7 mm in the anterior circulation in patients without previous rupture is zero.[1] However, several investigators have concluded that the risk of rupture for aneurysms less than 7 mm is significantly higher than stated by the International Study of Unruptured Intracranial Aneurysms (ISUIA) investigators.[2-4] In addition, the relationship between factors such as aneurysmal sac morphology, flow dynamics, and risk of hemorrhage has not been established. One strategy to decrease the morbidity and mortality associated with subarachnoid hemorrhage (SAH) is to predict which aneurysms are at higher risk of rupture and treat them early.

There is a growing interest in the use of physiologic data to improve the characterization of aneurysms. Numerous investigators have explored the impact of flow in relationship to aneurysm morphology by using techniques such as digital subtraction angiography (DSA)[5-14] and computational flow dynamics (CFD).[15-20] However, these methods require an invasive procedure. Newer, MR-based noninvasive techniques are showing promise in yielding similar anatomic information with additional benefit of quantitative and qualitative flow and pressure parameters. We have recently developed a novel MR phase contrast (PC) sequence called vastly undersampled isotropic projection reconstruction (VIPR).[21] The obtained data from PC-VIPR can be graphically processed to yield fluid streamline and velocity vector plots. Using fluid relationships, we can process the data to yield dynamic pressures.

PC-VIPR could potentially be used in the clinical setting to provide both qualitative and quantitative intra-aneurysmal hemodynamic information and help predict the risk for aneurysmal rupture with noninvasive means. The purpose of our study was to demonstrate that PC-VIPR could accurately assess intra-aneurysmal pressure gradients in a canine aneurysm model when compared with invasive measurements.

Materials and Methods

Canine Aneurysmal Model and Angiography

The Institutional Animal Care Use Committee approved the protocol for the study. Eight female beagles weighing approximately 30 pounds underwent surgery for the creation of 8 bifurcation and 8 sidewall aneurysms.[22] Of the 8 sidewall aneurysms, 3 had occluded. Therefore, we investigated 5 sidewall aneurysms in this study. All 8 bifurcation aneurysms were patent and used in this study. The aneurysm venous

Received December 24, 2006; accepted after revision March 12, 2007.

From the Departments of Neurosurgery (R.M., B.A.-K., P.A.T., A.S.T., D.B.N.), Radiology (B.A.-K., P.A.T., A.S.T., D.B.N., D.C., J.G., O.W., C.A.M.), and Medical Physics (K.J., O.W., C.A.M.); University of Wisconsin Hospital and Clinics, Madison, Wis.

Previously presented in part at: Annual Meeting of the American Society of Neuroradiology, May 5, 2006; San Diego, Calif.

Please address correspondence to Beverly Aagaard-Kienitz, MD, Department of Radiology, University of Wisconsin E3/311 CSC, 600 Highland Ave, Madison, WI 53792-325; e-mail: baagaard-Kienitz@uwhealth.org

DOI 10.3174/ajnr.A0648

pouch model has already been described in previous studies from our laboratory.[23]

With the animals under general anesthesia, we performed a digital subtraction angiogram (DSA) in the anteroposterior and oblique projections using standard techniques. The presence of the bifurcation and sidewall aneurysms was confirmed, followed by measurement of the height and width of the aneurysmal sac and neck. An Echelon 10 microcatheter (ev3, Irvine, Calif) was then advanced under fluoroscopy into the right common carotid artery proximal to the aneurysms in all cases. The microcatheter was connected to a Propaq arterial pressure monitor (Protocol Systems, Beaverton, Ore) and used to measure mean arterial pressure (MAP) in the parent vessel, aneurysm neck, and 5 regions within the aneurysmal sac. The 5 regions in each aneurysmal sac were designated as time on a clock face. Measures were taken at the 12, 3, 5, 7, and 9 o'clock positions so that pressure measurements were performed at approximately the same location in each aneurysm. Three separate pressure measurements were recorded from the microcatheter at every location. Appropriate pressure waveforms were verified before each pressure measurement was recorded. We observed systolic, diastolic, and mean arterial pressures for a period of 2 minutes to ensure stability of the reading before recordings were taken. MAP pressure measurements with the microcatheter technique have been validated against direct in vivo RD wire measurements in previous research (unpublished data). In the RD wire technique, a pair of 200-cm length 0.014-inch pressure-sensing guidewires (PressureWire 4; RD Medical Systems, Uppsala, Sweden) were connected to interface units (RD PressureWire Interface Unit). Each interface unit was connected to an analog to digital converter (LabJack U12; LabJack, Lakewood, Colo), which was then connected to a standard laptop personal computer (Windows XP; Microsoft, Redmond, Wash) running data acquisition software (LabVIEW, version 7; National Instruments, Austin, Tex). Before acquiring pressure measurements, we calibrated the wires and the patient monitoring system. In our previous research, we performed RD wire measurements across stenoses and directly compared them with microcatheter pressure measurements, with good correlation.

We calculated the intra-aneurysmal and parent vessel pressures as the mean of the 3 MAP readings obtained at each location. Subsequently, for every MAP in the aneurysm, we calculated a pressure differential by subtracting the MAP at that position from the MAP of the parent vessel.

PC-VIPR

Immediately after DSA, the catheter was removed, and each animal, while still under anesthesia, was placed in a 4-channel knee coil and imaged with a clinical 1.5T MR imaging scanner (TwinSpeed Excite HD, version 12.0; GE Healthcare, Waukesha, Wis). ECG leads were attached to the animals' chest for cardiac gating. Immediately after a contrast-enhanced MR angiogram was obtained, PC-VIPR data were then acquired with ECG gating at the following parameters: TE/TR of 3.4/8.8 ms, 256 × 256 × 256 acquisition matrix, 20 × 20 × 20 cm FOV, 32 kHz receiver bandwidth, 75% fractional readout, and a velocity encoding of 150 cm/s. Total imaging time for the PC-VIPR examination was 10 minutes. The voxel size of the PC-VIPR examination was 0.78 mm × 0.78 mm × 0.78 mm (0.48 mm^3). Data at individual timeframes within the cardiac cycle were reconstructed with use of an adaptive width temporal filter. The temporal width of this filter smoothly transitioned from 35.2 ms at the center of the *k*-space to 105.2 ms at the edges of the *k*-space sphere, where the sampling attenuation is reduced. This filter is more efficient than standard view sharing, allowing for higher temporal resolution of low-frequency components. For each timeframe, dynamic velocity images were reconstructed via phase difference processing. Images of vascular anatomy were generated from composite complex difference and magnitude volumetric dataset.

We then analyzed dynamic phase difference images to determine flow rates and pressure gradients. We then measured flow rates from the PC-VIPR data at the neck and left and right outflows tracts using a standard GE flow analysis package on the axial flow images. Pressure gradients were determined from iterative methods, which have been validated in both phantom and animal models to provide relatively accurate answers.[11,24-27] This technique is based on the Navier-Stokes equation, which simplifies more complex relationships by assuming the fluid to be both incompressible and Newtonian. Arterial blood flow generally satisfies these assumptions with a dynamic viscosity of approximately 4 cP (centipoise). A 4-step process was used in the implementation of the technique, consisting of vessel segmentation, pressure gradient determination, integrative pressure determination, and iterative refinement. Vessel segmentation was accomplished with a user-defined threshold, which was followed by an anti-island filter. This filter smoothed the vessel wall and removed small, isolated regions that could cloud images and introduce additional error. We then determined pressure gradients by using central difference equations with corrections for errors occurring at the edge of the vessel. We then determined an initial pressure map by using a simple seed point method. Subsequent to that, we iteratively refined this pressure map by using a path-averaging algorithm.[11,24-27] Dynamic pressure maps were then averaged for comparison with in vivo measurements, and pressure differences were compared on a pressure map registered to DSA images.

Data Evaluation and Statistics

The DSA images were reviewed, and the size of the aneurysms (including the neck) was recorded. The 3 catheter MAP measurements were averaged and compared to estimate the standard error in the catheter measurement and provide a comparison value with respect to pressure measurements derived from PC-VIPR data. Because localization of the catheter was performed with a single coronal plane, the expected value is the average pressure along the projection. To provide a correlative measure, we projected the 3D PC-VIPR pressure measurements in the same plane and divided them by the number of segmented pixels along the projection. This approach allows for measurements to be made in the same manner as those from the DSA. Each positional pressure measurement was matched with a corresponding PC-VIPR measurement and recorded at the same location on the basis of DSA registration.

Statistics

We correlated the time-averaged PC-VIPR pressure gradient measurements with the actual time-averaged pressure gradients (catheter measurement) by using a regression analysis and linear Bland-Altman analysis.

Results

In the 8 canines, we evaluated 8 bifurcation aneurysms and 5 sidewall aneurysms. The average size of the 8 bifurcation aneurysms was 11 mm × 7 mm with an average neck size of 4.8 mm. The average size of the 5 sidewall aneurysms was 9 mm x 7 mm with an average neck size of 5 mm. Using PC-VIPR, we obtained high-quality anatomic images as well as time-re-

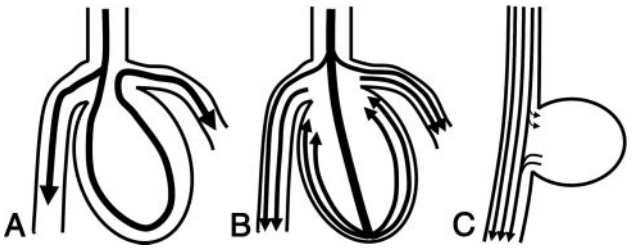

Fig 1. The 3 patterns of blood flow observed in the experimental aneurysms are illustrated: (*A*) recirculation pattern in bifurcation aneurysm, (*B*) jet pattern in bifurcation aneurysm, and (*C*) low flow pattern in sidewall aneurysm.

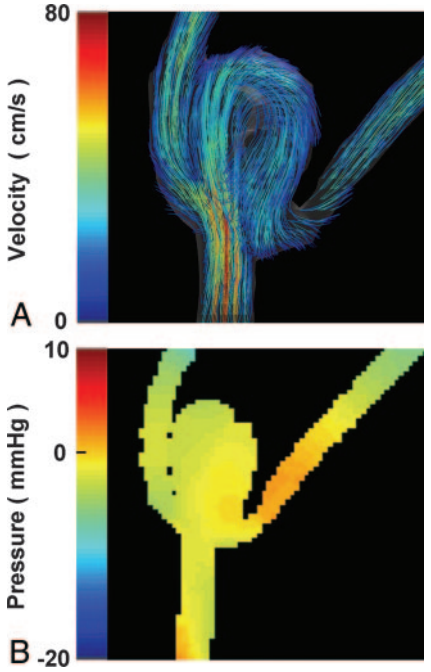

Fig 2. A recirculation blood-flow pattern is observed in these experimental bifurcation aneurysms. *A*, PC-VIPR imaging demonstrates the recirculation blood flow pattern. *B*, The PC-VIPR pressure map demonstrates a relatively low neck-to-dome pressure differential with recirculation-type blood flow pattern.

solved velocity maps, which were processed to yield velocity vector plots and pressure maps.

In the bifurcation and sidewall aneurysms, 3 main flow patterns were demonstrated, which are shown schematically in Fig 1. In 7 of the 8 bifurcation aneurysms, a recirculation blood flow pattern was observed (Fig 2). We defined recirculation pattern as blood flow that enters through a channel in the aneurysmal neck, circulates in the periphery of the sac, and subsequently exists the neck through a separate channel. This flow pattern resulted in a relatively low dome pressure gradient (mean, +0.5 mm Hg) (Fig 2). A jet blood-flow pattern was observed in a single case of bifurcation aneurysm (Fig 3). Jet pattern is defined as blood flow that enters the aneurysm neck through a channel, directly strikes the dome of the aneurysm, and then scatters and exits the neck of the aneurysm. The jet flow pattern resulted in a high dome pressure gradient (+50.2 mm Hg) (Fig 3). In all of the sidewall aneurysms, a low flow pattern was seen, resulting in an intermediate dome pressure gradient (mean, +8.3) (Fig 4).

To demonstrate the degree of correlation between the PC-VIPR pressure gradient measurements and the actual catheter pressure differential measurements, we performed regression analysis and linear Bland-Altman analysis. Both methods demonstrated a high degree of correlation ($R = 0.82$, $P < .01$) between the pressure measurements obtained with PC-VIPR and the catheter (Fig 5).

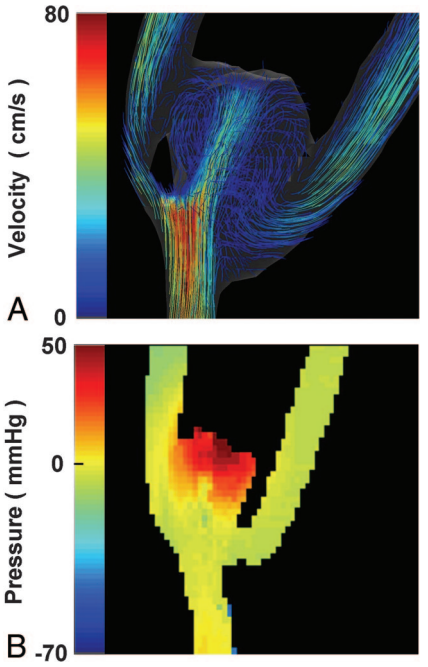

Fig 3. A jet blood-flow pattern is observed in a single case of bifurcation aneurysm. *A*, This bifurcation aneurysm demonstrates the jet blood-flow pattern with PC-VIPR imaging. *B*, The PC-VIPR pressure map of the aneurysm with the jet blood-flow pattern demonstrating the relatively high neck-to-dome pressure differential.

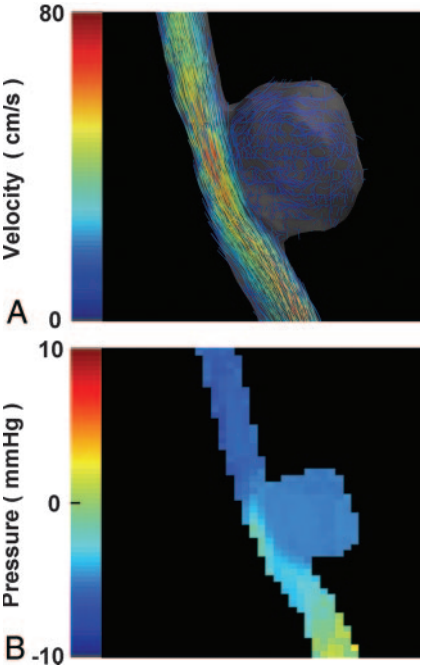

Fig 4. In the sidewall aneurysms, a pattern of low blood flow is seen, resulting in an intermediate dome pressure gradient. *A*, The low flow pattern is demonstrated with PC-VIPR. *B*, PC-VIPR pressure map of the aneurysm with low flow pattern demonstrating a relatively intermediate neck-to-dome pressure differential.

Discussion

The retrospective arm of the ISUIA concluded that the risk of rupture of an aneurysm smaller than 10 mm in a patient with no previous SAH is 0.05%.[28] Subsequent to that, the prospective arm of the ISUIA concluded that the 5-year cumulative rates of rupture for aneurysms in the anterior circulation in patients with no previous SAH was 0% in aneurysms less than 7 mm and 2.5% in aneurysms of the posterior circulation.[1] In addition, taking into account the incidence and prevalence for both unruptured intracranial aneurysms and SAH, the ISUIA data imply that almost 1 in 6 patients older than 30 years would harbor an incidental unruptured aneurysm.[2] The discrepancy between the ISUIA and other studies implies that predicting which aneurysms are more likely to rupture may not be as simple as taking into consideration the aneurysm size, location, and previous rupture and that perhaps additional criteria must be investigated.

Aneurysmal hemodynamics are thought to be an important factor in pathogenesis and thrombosis.[10,12,14,29,30] Hemodynamic data such as intra-aneurysmal pressure and flow dynamics could potentially be used as an additional set of criteria to assess the risk of aneurysmal rupture. Defining aneurysms from a physiologic standpoint is topic of several studies.[13,15,18,19,31] Most of these investigations are performed in CFD models, which inherently possess several limitations such as assumptions on the distribution of elasticity and wall thickness and blood flow as an incompressible Newtonian flow. In addition, CFD requires DSA data, an invasive procedure, whereas PC-VIPR is noninvasive.

VIPR is a novel PC MR technique that radially undersamples the *k*-space, resulting in improved resolution from inherent oversampling of the central *k* space.[21] This culminates in isotropic data acquired significantly faster than standard Cartesian methods. The clinical consequence of this is that in a single examination, both anatomic and physiologic data could be available. PC-VIPR has the greatest potential in assessing patients with unruptured aneurysms because it provides anatomic, qualitative as well as quantitative intra-aneurysmal pressure and flow data throughout the cardiac cycle in a noninvasive fashion. The qualitative and quantitative data can potentially be used as additional criteria to assess risk of aneurysmal rupture. Another advantage of PC-VIPR is that images can be acquired within minutes as part of a diagnostic noninvasive imaging study, which would be critical in the clinical setting.

In this study, we applied PC-VIPR to canine aneurysmal models to assess the potential for obtaining anatomic and physiologic data. PC-VIPR provided flow velocity vector as well as pressure gradient maps in both bifurcation and sidewall aneurysmal models of different sizes. In one of the bifurcation aneurysms, a jet flow pattern into the aneurysm was observed. This was different from the recirculation pattern, which was observed in the other 7 bifurcation aneurysms. In the jet flow pattern, the aneurysmal dome pressure was significantly higher than that in the recirculation pattern (+50.2 mm Hg vs +0.5 mm Hg). The significance of the jet flow pattern with a higher dome pressure versus the recirculation pattern with a lower dome pressure in an aneurysmal rupture needs to be evaluated in the clinical setting. However, one could speculate that aneurysms with a jet flow pattern against an aneurysmal dome with a higher dome pressure could have a higher risk of rupture than aneurysms with a recirculation pattern. The recirculation pattern would theoretically be associated with higher shear stress at the aneurysmal dome because the blood dragging against the wall causes higher frictional force. On the other hand, the jet flow pattern would be theoretically associated with low shear stress because the blood strikes the dome and scatters. In this case, there would be less degree of friction against the aneurysmal wall. This theory would be supported by other studies,[17,32] which have shown that the areas of the aneurysmal rupture are associated with lower shear wall stress. In the 5 sidewall aneurysmal models, the flow was low. In theory, the pressure of the dome in those aneurysms should be small, which was confirmed in this study. The importance of low flow and dome pressure in sidewall aneurysms and risk of rupture needs to be studied further.

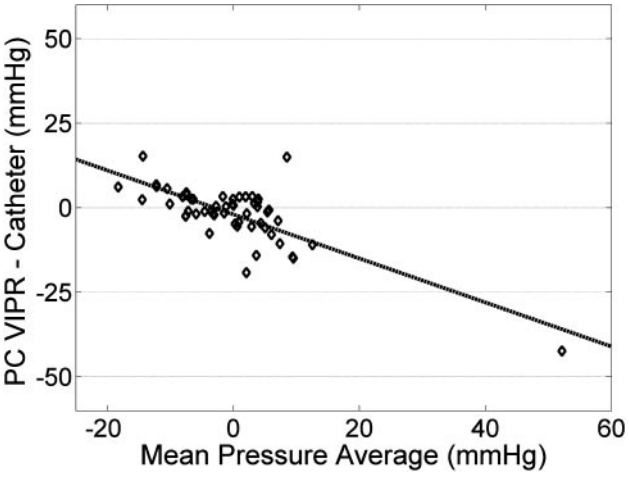

Fig 5. The linear Bland-Altman analysis demonstrates the high correlation between the PC-VIPR and catheter pressure measurements. The x-axis is the average of PC-VIPR and catheter pressure measurements, and the y-axis is the difference between the PC-VIPR and catheter pressure measurements.

Using a catheter-based technique, we measured intra-aneurysmal pressures and compared them with PC-VIPR. There was a high degree of correlation ($R = 0.82$, $P < .01$) between pressures obtained noninvasively with PC-VIPR and invasively with the microcatheter. The high degree of correlation supports PC-VIPR as a tool that could potentially be used in the clinical setting to categorize unruptured aneurysms on the basis of their hemodynamic characteristics.

One of the limitations of this study was that the aneurysmal wall in the canine model was venous, which may behave differently from arterial aneurysms. Another weakness of this work was that some of the 3 intra-aneurysmal catheter-based pressures demonstrated some variability. The statistical uncertainty of a single catheter measurement was found in this study to be around 6 mm Hg, likely because of inaccuracies in repositioning. The position of the catheter in the aneurysmal sac was based on the 2D DSA image. Therefore, each measurement in the aneurysmal sac might not have been in the same 3D location, leading to variability in pressure readings. Because all measurements of microcatheter pressure were MAPs, the problem of capturing some pressures in systole and others in diastole should not have been an issue. In a previous related study at our institution, the authors validated PC-VIPR mea-

surements across a carotid stenosis model using the microcatheter method for pressure measurements.[33] Another potential source of error in this study was the presence of a time delay (approximately 1 hour) between the microcatheter and PC-VIPR pressure measurements, which could have led to some degree of discrepancy between the 2 pressure measurements.

In future studies, we are planning to further investigate other hemodynamic parameters, including shear stress in the canine aneurysmal model and in human aneurysms. With the validation of PC-VIPR to provide accurate qualitative as well as quantitative hemodynamic data in aneurysms, we may be able to noninvasively identify physiologic criteria that could predict aneurysms with higher risk of rupture.

Conclusion

The PC-VIPR sequence can provide high-quality images of vascular anatomy as well as accurate physiologic information of experimental aneurysms. Qualitative and quantitative flow velocity vector and pressure maps were obtained in the canine aneurysm model. The noninvasive aneurysmal pressures provided by PC-VIPR were validated by invasive microcatheter pressure measurements. Application of this novel MR technique to clinical human cases of unruptured and ruptured aneurysms, as well as assessment of wall shear stress, is currently being evaluated.

References

1. Wiebers DO, Whisnant JP, Huston J 3rd, et al. **Unruptured intracranial aneurysms: natural history, clinical outcome, and risks of surgical and endovascular treatment**. *Lancet* 2003;362:103–10
2. Winn HR, Jane JA Sr, Taylor J, et al. **Prevalence of asymptomatic incidental aneurysms: review of 4568 arteriograms.** *J Neurosurg* 2002;96:43–49
3. Juvela S, Porras M, Poussa K. **Natural history of unruptured intracranial aneurysms: probability of and risk factors for aneurysm rupture.** *J Neurosurg* 2000;93:379–87
4. Juvela S, Porras M, Heiskanen O. **Natural history of unruptured intracranial aneurysms: a long-term follow-up study.** *J Neurosurg* 1993;79:174–82
5. Sorteberg A, Sorteberg W, Rappe A, et al. **Effect of Guglielmi detachable coils on intraaneurysmal flow: experimental study in canines** [published erratum appears in *AJNR Am J Neuroradiol* 2002;23:742]. *AJNR Am J Neuroradiol* 2002;23:288–94
6. Sorteberg A, Sorteberg W, Aagaard BD, et al. **Hemodynamic versus hydrodynamic effects of Guglielmi detachable coils on intra-aneurysmal pressure and flow at varying pulse rate and systemic pressure.** *AJNR Am J Neuroradiol* 2004;25:1049–57
7. Imbesi SG, Kerber CW. **Analysis of slipstream flow in a wide-necked basilar artery aneurysm: evaluation of potential treatment regimens.** *AJNR Am J Neuroradiol* 2001;22:721–24
8. Kerber CW, Liepsch D. **Flow dynamics for radiologists. II. Practical considerations in the live human.** *AJNR Am J Neuroradiol* 1994;15:1076–86
9. Kerber CW, Liepsch D. **Flow dynamics for radiologists. I. Basic principles of fluid flow.** *AJNR Am J Neuroradiol* 1994;15:1065–75
10. Strother CM, Graves VB, Rappe A. **Aneurysm hemodynamics: an experimental study.** *AJNR Am J Neuroradiol* 1992;13:1089–95
11. Thompson RB, McVeigh ER. **Fast measurement of intracardiac pressure differences with 2D breath-hold phase-contrast MRI.** *Magn Reson Med* 2003;49:1056–66
12. Isoda H, Hirano M, Takeda H, et al. **Visualization of hemodynamics in a silicon aneurysm model using time-resolved, 3D, phase-contrast MRI.** *AJNR Am J Neuroradiol* 2006;27:1119–22
13. Cebral JR, Castro MA, Appanaboyina S, et al. **Efficient pipeline for image-based patient-specific analysis of cerebral aneurysm hemodynamics: technique and sensitivity.** *IEEE Trans Med Imaging* 2005;24:457–67
14. Mantha A, Karmonik C, Benndorf G, et al. **Hemodynamics in a cerebral artery before and after the formation of an aneurysm.** *AJNR Am J Neuroradiol* 2006;27:1113–18
15. Steinman DA, Milner JS, Norley CJ, et al. **Image-based computational simulation of flow dynamics in a giant intracranial aneurysm.** *AJNR Am J Neuroradiol* 2003;24:559–66
16. Metcalfe RW. **The promise of computational fluid dynamics as a tool for delineating therapeutic options in the treatment of aneurysms.** *AJNR Am J Neuroradiol* 2003;24:553–54
17. Shojima M, Oshima M, Takagi K, et al. **Magnitude and role of wall shear stress on cerebral aneurysm: computational fluid dynamic study of 20 middle cerebral artery aneurysms.** *Stroke* 2004;35:2500–05
18. Castro MA, Putman CM, Cebral JR. **Patient-specific computational modeling of cerebral aneurysms with multiple avenues of flow from 3D rotational angiography images.** *Acad Radiol* 2006;13:811–21
19. Hassan T, Timofeev EV, Saito T, et al. **A proposed parent vessel geometry-based categorization of saccular intracranial aneurysms: computational flow dynamics analysis of the risk factors for lesion rupture.** *J Neurosurg* 2005;103:662–80
20. Burleson AC, Strother CM, Turitto VT. **Computer modeling of intracranial saccular and lateral aneurysms for the study of their hemodynamics.** *Neurosurgery* 1995;37:774–82; discussion 782–84
21. Gu T, Korosec FR, Block WF, et al. **PC VIPR: a high-speed 3D phase-contrast method for flow quantification and high-resolution angiography.** *AJNR Am J Neuroradiol* 2005;26:743–49
22. German WB, Black SP. **Experimental production of carotid aneurysms.** *N Engl J Med* 1954;250:104–06
23. Graves VB, Ahuja A, Strother CM, et al. **Canine model of terminal arterial aneurysm.** *AJNR Am J Neuroradiol* 1993;14:801–03
24. Ebbers T, Wigstrom L, Bolger AF, et al. **Estimation of relative cardiovascular pressures using time-resolved three-dimensional phase contrast MRI.** *Magn Reson Med* 2001;45:872–79
25. Urchuk SN, Plewes DB. **MR measurements of pulsatile pressure gradients.** *J Magn Reson Imaging* 1994;4:829–36
26. Urchuk SN, Fremes SE, Plewes DB. **In vivo validation of MR pulse pressure measurement in an aortic flow model: preliminary results.** *Magn Reson Med* 1997;38:215–23
27. Yang GZ, Kilner PJ, Wood NB, et al. **Computation of flow pressure fields from magnetic resonance velocity mapping.** *Magn Reson Med* 1996;36:520–26
28. **Unruptured intracranial aneurysms–risk of rupture and risks of surgical intervention. International Study of Unruptured Intracranial Aneurysms Investigators** [published erratum appears in *N Engl J Med* 1999;340:744]. *N Engl J Med* 1998;339:1725–33
29. Ford MD, Stuhne GR, Nikolov HN, et al. **Virtual angiography for visualization and validation of computational models of aneurysm hemodynamics.** *IEEE Trans Med Imaging* 2005;24:1586–92
30. Kayembe KN, Sasahara M, Hazama F. **Cerebral aneurysms and variations in the circle of Willis.** *Stroke* 1984;15:846–50
31. Tateshima S, Grinstead J, Sinha S, et al. **Intraaneurysmal flow visualization by using phase-contrast magnetic resonance imaging: feasibility study based on a geometrically realistic in vitro aneurysm model.** *J Neurosurg* 2004;100:1041–48
32. Yamashita S IH, Takeda H, Okura Y, et al. **Analysis of wall shear stress of intracranial arteries using time-resolved three-dimensional phase contrast MR imaging: preliminary report.** [poster] American Society of Neuroradiology 44th Annual Meeting April 29-May 5, 2006
33. Turk AS, Johnson KM, Lum D, et al. **Physiologic and anatomic assessment of a canine carotid artery stenosis model utilizing phase contrast with vastly undersampled isotropic projection imaging.** *AJNR Am J Neuroradiol* 2007;28:111–15